



Additive-free vapour-phase hydrogenation of benzonitrile over MgO-supported Ni catalysts

A. Nagu^{1,2} · K. Vasikerappa^{1,2} · P. Gidyonu^{1,2} · Ch. Prathap^{1,2} · M. Venkata Rao² · K. S. Rama Rao² · B. David Raju²

Received: 11 November 2019 / Accepted: 25 February 2020

© Springer Nature B.V. 2020

Abstract

MgO-supported Ni catalysts were selectively catalysed by the hydrogenation of benzonitrile to benzylamine in continuous flow at atmospheric pressure without any additives. Ni/MgO catalysts were synthesized by co-precipitation method with NaOH as the precipitating agent. All the synthesized catalysts were characterized by various physiochemical techniques, namely XRD, H₂-TPR, BET surface area, CO₂-TPD, SEM, and TEM. Among them, 10% Ni/MgO catalyst showed the best activity with 98% conversion of benzonitrile, 60% selectivity to benzylamine at 473 K. The high dispersion of Ni and strong metal support interactions with MgO are key factors for the catalytic performance. 10Ni/MgO catalyst was found to be consistent throughout the time-on-stream studies of 36 h which clearly explains the excellence of the catalytic system.

Electronic supplementary material The online version of this article (<https://doi.org/10.1007/s11164-020-04113-y>) contains supplementary material, which is available to authorized users.

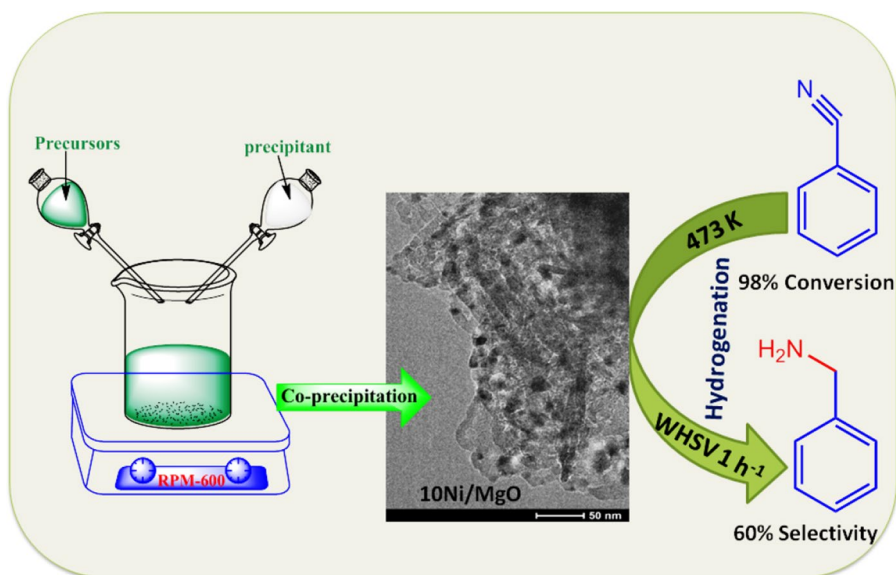
✉ B. David Raju
david@iict.res.in

¹ CSIR-Academy of Scientific and Innovative Research (CSIR-AcSIR), New Delhi, India

² Catalysis and Fine Chemicals Division, CSIR-Indian Institute of Chemical Technology, Hyderabad 500007, India

Graphic abstract

Ni/MgO catalysts are active in gas phase hydrogenation of benzonitrile to benzylamine at atmospheric pressure.



Keywords Benzonitrile · Benzylamine · Hydrogenation · Ni · MgO

Introduction

The chemo-selective hydrogenation of aromatic nitriles to amines is an imperative reaction due to the wide utility of amines in various industries, especially pharmaceutical and textile industries [1-4]. From the bibliographic standpoint, numerous studies were carried out for the hydrogenation of nitriles over both homogeneous and heterogeneous metal catalysts [5, 6]. Comparatively, homogeneous catalysts are effective in activity and selectivity, but involve tedious workup procedures, metal particle contamination and difficulty in recovery and reuse of catalyst and in addition, use of base additives create further problems [4]. For instance, Ru(cod) methylallyl₂-DPPF active catalyst at 50 bar of H₂ pressure in t-BuOK and toluene solvent give 99% selectivity to benzylamine [7]. 10Pd-C is an active catalyst under 6 bar of H₂ pressure in NaH₂PO₄ and dimethyl carbonate–water dual solvent [8]. RuCl₂(PPh₃)₃ catalyst showed the best results under a H₂ pressure of 50 bar in 24 h [9]. With the economic and environmental barriers, use of homogeneous catalysts can be abandoned. K. Lévy et al. published a detailed review on selective heterogeneous catalytic hydrogenation of nitriles to primary amines. They pointed out that the selective formation of primary amines is a challenging task. The selection of metal, metal support interactions, and reaction parameters are crucial for achieving

selectivity to primary amine [6]. Production of benzylamine from hydrogenation of benzonitrile over heterogeneous catalysts such as supported metal catalysts is considered as an atom-efficient route. However, hydrogenation of benzonitrile has been established at higher H₂ pressure (6–100 bar) [8, 10–16] over supported metal (Pt [15], Rh [15] Pd [10–17], and Ni [8, 18]) catalysts [19]. Pd-MCM-41 showed excellent activity with 91% conversion of nitrile and 90% selectivity of benzylamine at a partial pressure of H₂ and CO₂ of 20 and 100 bar, respectively [15]. Alumina-supported Pd catalyst is active towards hydrogenation of benzonitrile to benzylamine at 20 bar of H₂ pressure in 2-propanol solvent with 95% selectivity of benzylamine [10, 11]. Even with heterogeneous catalysts, pressurized H₂ operations and formation of by-products are still to be solved [12]. Various supported Cu [4], Ni [10, 11] and Pd [8, 12] metal catalysts were reported for the titled reaction at eco-friendly conditions [20]. Due to the low cost of nickel, supported Ni catalysts have been frequently used [21]. A Ni/Mo is one of the catalysts with 100% conversion and 99% selectivity in methanol solvent at 15 bar of hydrogen pressure [22]. RANEY's Ni catalyst showed 95% selectivity of benzylamine and 100% conversion of nitriles [23]. It is reported that the acidic sites favour the formation of tertiary and secondary amines, whereas basic sites selectively produce primary amines [4, 24]. Hence, use of basic supports to get selective production of primary amines is highly helpful. The abundant literature on benzonitrile to benzylamine confirming that the catalysts used involve: (1) use of expensive metal catalysts and solvents, (2) base additive requirement, (3) high H₂ pressure operations, (4) poor activity and selectivity, etc. leads to environmental and economic issues. At this juncture, development of inexpensive and eco-friendly catalysts with high activity and selectivity under mild operating conditions is an urgent requirement. Herein, Ni/MgO catalysts have been prepared, characterized, and used for the hydrogenation of benzonitrile (BN) to benzylamine (BA) under atmospheric pressure and obtained good activity and selectivity, which are delineated sequentially.

Experimental

Catalyst preparation

Ni/MgO catalysts with various Ni loadings of 5Ni/MgO, 10Ni/MgO, 15Ni/MgO, and 20Ni/MgO (in wt%) have been prepared by co-precipitation method [25]. Ni (NO₃)₂·6H₂O (M/s. Alfa Aesar, USA 99.9%) and Mg (NO₃)₂·6H₂O (M/s. Loba Chemie, India Assay 99.5%) were used as precursors of Ni/MgO catalysts. Precursors were mixed together in 1000 mL distilled water, and the mixed solution precipitated at pH 9.0 by the addition of 0.5 M aqueous solution of NaOH (M/s. Loba Chemie, India). The precipitation is filtered and washed ten times with 2000 mL of distilled water in order to remove the sodium ions, dried at 393 K for 12 h. Finally, the dried sample is calcined in static air at 773 K for 5 h and prior to the reaction the catalysts were reduced in H₂ flow at 873 K for 4 h. The prepared catalysts were designated as 5Ni/MgO, 10Ni/MgO, 15Ni/MgO, and 20Ni/MgO where the prefixed numerical value indicates the weight percentage of Ni loading on the MgO support.

Characterizations of catalysts

X-ray diffraction (XRD) patterns have been recorded (after ex-situ reduction of the catalysts) on Ultima-IV (M/s. Rigaku Corporation, Japan), XRD unit was operated at 40 kV and 40 mA equipped with Ni-filtered Cu K α radiation ($\lambda = 1.54056 \text{ \AA}$), and a 2θ value ranges from 20° to 80° at a scanning rate of 4° min^{-1} . N $_2$ physisorption studies have been carried out by using a Quadrasorb-SI (M/s. Quantachrome Instruments Corporation, USA) at liquid nitrogen temperature. Prior to the measurement, the sample was out-gassed at 473 K for 3 h. Temperature-programmed reduction (TPR) studies were acquired on a homemade equipment containing a quartz reactor with electrical heating and a thermal conductivity detector (TCD)-equipped gas chromatograph connected at the outlet of the reactor. About 50 mg of catalyst was placed at the centre of the quartz reactor between two plugs of quartz; wool was pre-treated at 573 K for 1 h in Ar flow (60 mL min^{-1}). Then the catalyst was exposed to 5% H $_2$ balance Ar gas flow for 1 h at 373 K followed by being raised to a temperature up to 1073 K at a heating rate of 10 K min^{-1} . The H $_2$ concentration was monitored by standard GC software. The total basicity of the catalysts has been measured by temperature-programmed desorption (TPD) of CO $_2$ using an AUTOSORB iQ automated gas sorption analyzer (M/s. Quantachrome Instruments, USA); 0.01 g of catalyst has been loaded and pre-treated in a He gas flow (99.8%, 50 mL min^{-1}) at 523 K for 1 h. After pre-treated catalysts were saturated with 10% CO $_2$ -helium at 323 K for 1 h, it was followed by flushing with helium gas for 1 h to flush off the physisorbed CO $_2$ at the same temperature. Then temperature to 1200 K at 10 K min^{-1} and desorbed CO $_2$ was monitored with the inbuilt TCD in a flow of helium (99.8%, 30 mL min^{-1}). SEM and TEM analyses were studied on scanning electron microscope (M/s. JEOL, Switzerland) and transmission electron microscope (M/s JEOL, Switzerland) operating between 160 and 180 kV, respectively. Before TEM analysis, the catalyst sample ultrasonication in ethanol and a drop was placed on a copper grid (carbon coated) and solvent was evaporated in air at 350 K for 5 h.

Catalyst activity test

Gas-phase selective hydrogenation of benzonitrile was studied in a fixed-bed quartz reactor (14 mm id and 300 mm length) at atmospheric pressure in the temperature range of 453–513 K; 1 g of catalyst was sandwiched at the middle of quartz reactor in between two quartz wool layers, with dilution of quartz grains, and catalyst was reduced at 873 K under the H $_2$ flow rate of 40 mL h^{-1} for 4 h. Reaction temperature was fixed, and benzonitrile was fed at a flow rate of 1 mL h^{-1} by using a syringe feed pump (M/s. B. Braun, Germany) along with H $_2$ (99.5% pure) flow of 30 mL min^{-1} . The product mixture was collected in an ice-cooled trap at every interval and product mixture identified by an FID-equipped gas chromatograph, GC-17A (Equity-5 capillary column

(30 m × 0.53 mm × 5.0 μm), M/s. Shimadzu Instruments, Japan) and confirmed by GC–MS, QP-2010 (EB-5MS capillary column (30 m × 0.25 mm × 0.25 μm) M/s. Shimadzu Instruments, Japan).

$$\text{Conversion (\%)} = \frac{\text{Moles of reactant}_{\text{in}} - \text{Moles of reactant}_{\text{out}}}{\text{Moles of reactant}_{\text{in}}} \times 100$$

$$\text{Selectivity (\%)} = \frac{\text{Moles of product formed}}{\text{Moles of reactant converted}} \times 100$$

Results and discussion

Brunauer–Emmett–Teller (BET) surface areas of prepared catalysts are shown in Table 1. The surface area of MgO is more than that of Ni/MgO catalysts. As metal content increases, the surface area of catalysts is decreased due to the pore blockage of the support. The results are in accordance with results reported in the literature [26–28].

X-ray diffraction (XRD) patterns of calcined Ni/MgO catalysts, NiO, and MgO support (prepared by the same method) are depicted in Fig. 1. Support MgO and NiO not only exhibited similar diffraction patterns but also showed nearby characteristic peaks because both NiO and MgO have similar ionic radii and the same rock salt structure [29, 30]. All Ni/MgO catalysts exhibited the same XRD patterns before the reduction. There are no distinguishable peaks of NiO identified in Ni/MgO catalysts. It should be observed that support MgO and NiO have similar patterns without doublet structure, indicating that NiO–MgO mixed oxide formed during the calcination [31]. This NiO–MgO mixed oxide acts as sources of small Ni⁰ particles [32–34]. The peaks located at 2θ of 36.93°, 43.04°, 62.47°, 74.97°, and 78.91° in the XRD patterns of Ni/MgO catalysts contribute to the formation of NiO–MgO mixed oxide. Figure 2 shows the XRD patterns of reduced Ni/

Table 1 Physico-chemical properties of the catalysts

Catalyst	^a Surface area (m ² g ⁻¹)	^b Crystallite size of Ni (111) nm	^c Hydrogen consumption (μmol g ⁻¹)	^d Total basicity (μmol CO ₂ g ⁻¹)
MgO	118	–	–	478
5Ni/MgO	98	5.2	214	463
10Ni/MgO	88	7.2	253	448
15Ni/MgO	76	9.5	288	410
20Ni/MgO	62	12	358	378

^aCalculated from BET

^bCalculated from XRD

^cCalculated from TPR

^dCalculated from TPD of CO₂

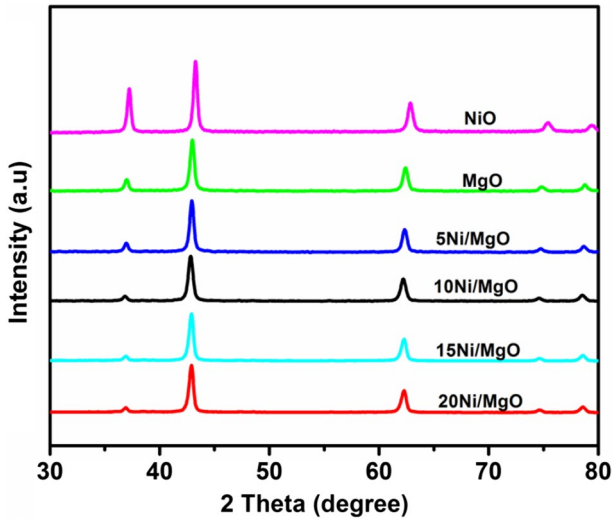


Fig. 1 XRD patterns of calcined Ni/MgO catalysts, NiO, and MgO support

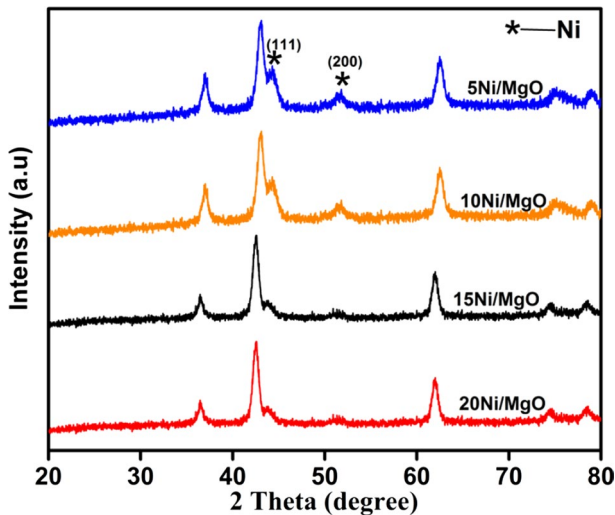


Fig. 2 XRD patterns of reduced Ni/MgO catalysts

MgO catalysts at 873 K for 4 h. After reduction, three metallic nickel diffraction peaks were detected at 44.49 (111), 51.89 (200), and 76.38 (220) (JCPDF 87-0712). The peaks around $2\theta = 42.88^\circ$, 36.99° , 62.28° , 76.18° , and 78.98° correspond to crystalline-phase MgO or solid solution of NiO–MgO on 2θ scale. The increase in crystallite size of metallic Ni (111) with increase in nickel loading and obtained results are shown in Table 1.

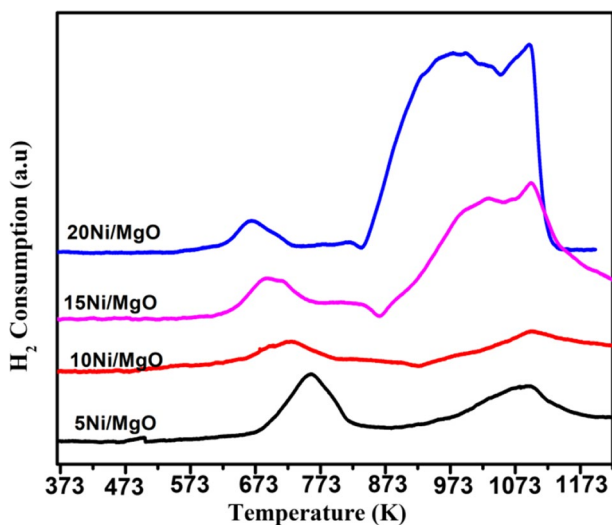


Fig. 3 H_2 -TPR patterns of Ni/MgO catalysts

Temperature-programmed reduction (H_2 -TPR) patterns of Ni/MgO are depicted in Fig. 3. It can be inferred from Fig. 3 that the TPR patterns of the 5Ni/MgO and 10Ni/MgO catalysts exhibited two reduction peaks with T_{\max} at 761, 1083, and 729, 1096 K, respectively. On the other hand, for 15Ni/MgO and 20Ni/MgO catalysts, three reduction peaks with T_{\max} 696, 1026, 1098 K and 669, 983, 1093 K, respectively, were also observed. The reduction peaks attributed to the reduction of NiO located on the MgO surface; in the outermost layer of the MgO structure, some Ni^{2+} ions possess square-pyramidal coordination and the NiO–MgO ($MgNiO_2$) mixed oxide lattice [35], respectively. The defect sites of MgO are responsible for strongly adsorbed nickel species on MgO [26]. Zecchina et al. reported that the NiO–MgO mixed oxides reduced in the temperature range 671–1093 K are mainly the Ni^{2+} ions located on the surface, and at temperature higher than 1093 K Ni^{2+} located in the bulk could be reduced [31]. Therefore, metallic Ni was originated from Ni^{2+} ions presented over surface of NiO–MgO mixed oxide in our catalysts. NiO–MgO mixed oxide solution is achieved during the calcination [30].

Temperature-programmed desorption of CO_2 (CO_2 -TPD) is a well-known technique to determine the total basicity of solid catalysts; the respective CO_2 -TPD profiles of MgO and Ni/MgO catalysts are displayed in Fig. 4. All the catalysts displayed a similar distribution of basic sites with T_{\max} in the range of 430 K, 650 K, and 873 K. The desorption peaks in the temperature range of 373–523 K represent the presence of weak basic sites, and 523–773 K and 773–973 K indicate the presence of moderate and strong basic sites, respectively. As metal loading increases, the moderate basic sites are increased. Alternatively, the strong basic sites are decreased.

The morphological features of the 10Ni/MgO catalyst were studied on scanning electron microscopy (SEM) and transmission electron microscopy (TEM) techniques. The images of SEM and TEM are displayed in Fig. S1 and Fig. 5.

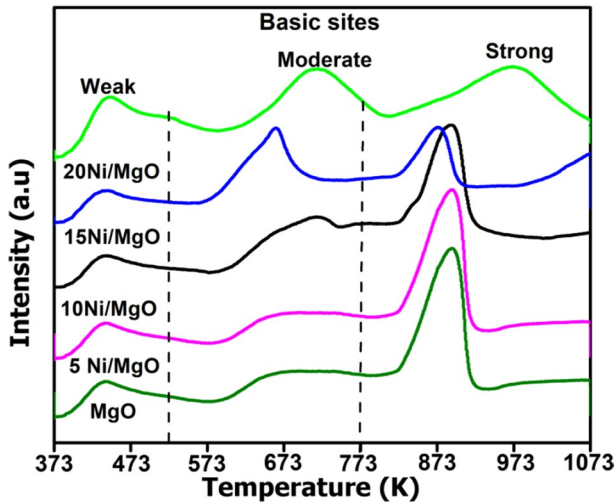


Fig. 4 CO_2 -TPD of MgO and Ni/MgO catalysts

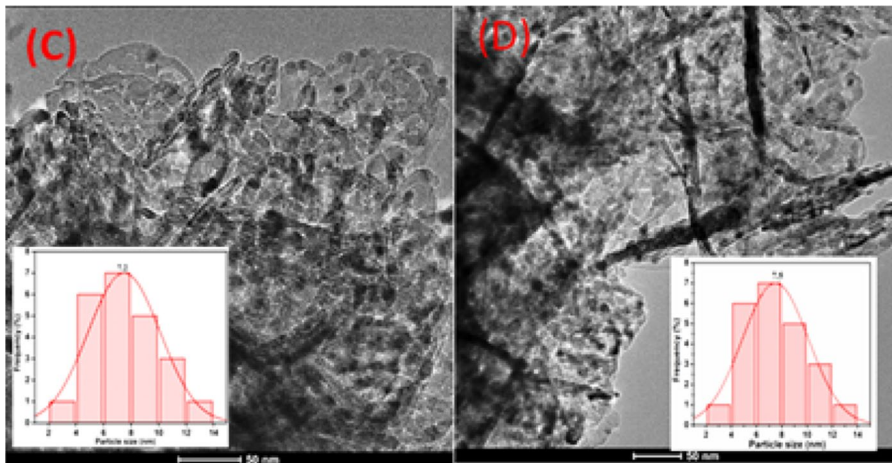


Fig. 5 a TEM image of reduced 10Ni/MgO and b TEM image of used 10Ni/MgO catalyst

SEM images of 10Ni/MgO catalyst show smooth surfaces of MgO in support and MgO-supported Ni catalyst. TEM image of reduced 10Ni/MgO catalyst indicated well-distributed Ni particles with an average particle size of 7.2 nm which is consistent with the XRD results, and TEM image of used 10Ni/MgO catalyst exhibited Ni particles with an average particle size of 7.5 nm.

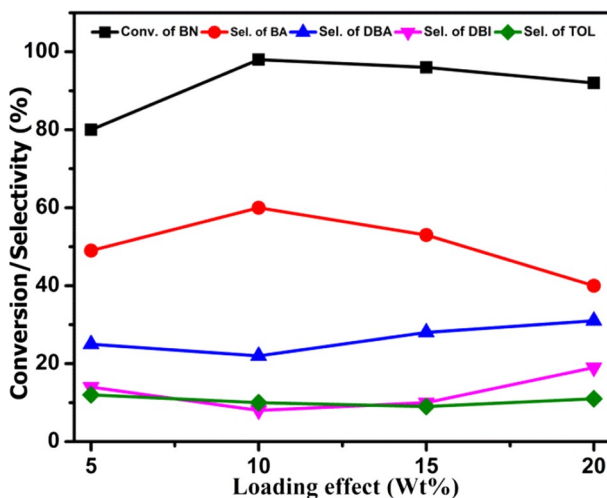


Fig. 6 Influence of nickel loading for the hydrogenation of benzonitrile. Reaction conditions: catalyst weight 1 g, feed 1 mL/h, temperature 473 K, pressure 1 atm, and $H_2/BN=8$ (molar ratio)

Activity studies

The vapour-phase hydrogenation of benzonitrile was studied over MgO-supported Ni catalysts, and the results are presented in Fig. 6. Scheme 1 represents probable reaction path ways during the hydrogenation of benzonitrile. This reaction involves hydrogenation, condensation, and hydrogenolysis reactions that can yield benzylamine (BA), *N*-benzylidenebenzylamine (DBI), dibenzylamine (DBA), and toluene (TOL), respectively; ammonia (NH_3) is eliminated during condensation reaction and hydrogenolysis to toluene [9].

The conversion of BN and selectivity to BA is increased with nickel loading from 5 to 10 wt% and reaches a maximum BN conversion of 98% with 60% selectivity to BA at 473 K over 10Ni/MgO catalyst. Further with increase in nickel loading from 10 to 20 wt%, there is a reverse trend in both conversions of BN and selectivity to BA. These results can be attributed to the formation of larger Ni particles over MgO in 15Ni/MgO and 20Ni/MgO catalysts that decrease the activity and selectivity in the vapour-phase hydrogenation of BN. The activity results are found to be in the order: 10Ni/MgO > 15Ni/MgO > 5Ni/MgO > 20Ni/MgO.

The effect of reaction temperature on the best catalyst 10Ni/MgO was conducted at different temperatures, viz. 453, 473, 493, and 513 K, and the results are presented in Fig. 7. As reaction temperature increased, the conversion of BN is enhanced while the selectivity to BA is increased with reaction temperature up to 473 K; beyond this, the selectivity to BA shows a downfall. The increase in reaction temperature promotes the formation of other products through over-hydrogenation and hydrogenolysis reactions. The maximum selectivity to BA is 60% obtained at 473 K with 98% conversion of BN.

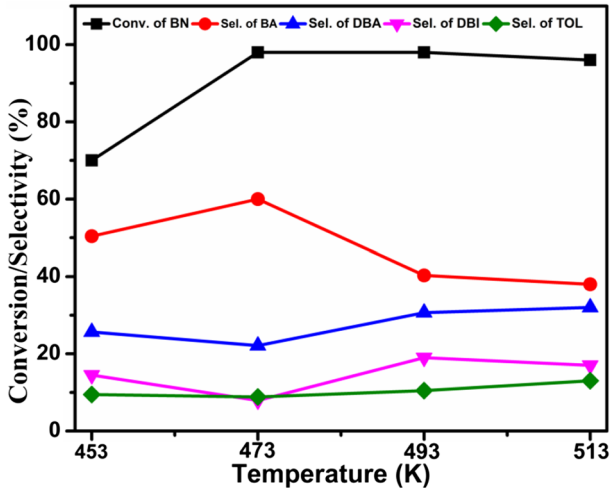


Fig. 7 Influence of temperature on the hydrogenation of benzonitrile on 10Ni/MgO catalyst. Reaction conditions: catalyst weight 1 g, feed 1 mL/h, pressure 1 atm, $H_2/BN = 8$ (molar ratio)

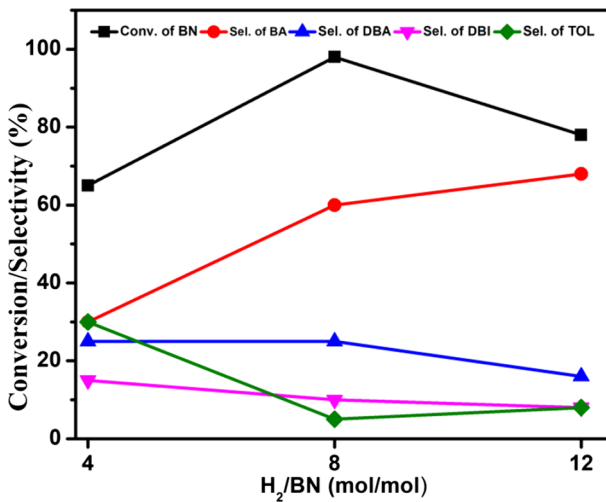


Fig. 8 Influence of hydrogen molar ratio on BN over 10Ni/MgO catalyst. Reaction conditions: temperature 473 K, pressure 1 atm, catalyst weight 1 g, feed 1 mL h⁻¹

The vapour-phase hydrogenation of BN was studied over 10Ni/MgO catalyst at 473 K under different BN/ H_2 mole ratios to understand the optimum H_2 moles needed to convert BN to BA (Fig. 8). In general, one mole of BN requires two moles of hydrogen to produce one mole of BA. The studies were carried out using different BN/ H_2 molar ratios such as 1:4, 1:8, and 1:12. At initial BN/ H_2 molar ratio (1:4), 65% conversion of BN with 30% selectivity of BA and 29% of TOL is formed. With

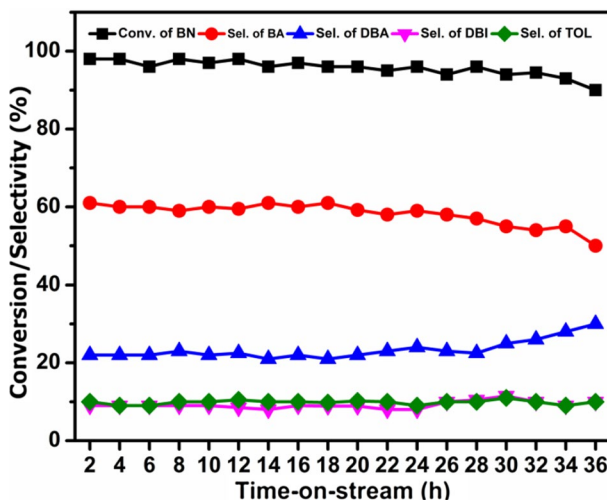
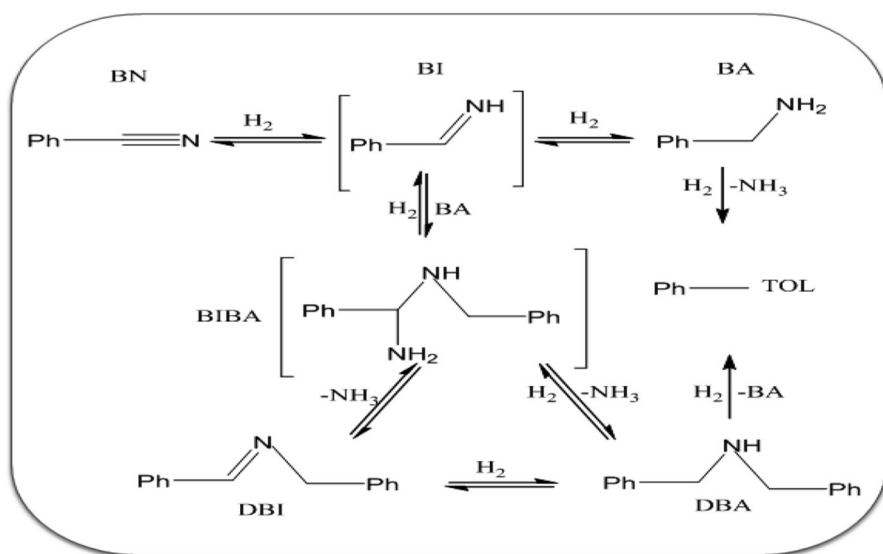


Fig. 9 Time-on-stream study for the hydrogenation of benzonitrile on 10Ni/MgO catalyst. Reaction conditions: catalyst weight 1 g, feed 1 mL/h, temperature 473 K, pressure 1 atm, $H_2/BN=8$ (molar ratio)



Scheme 1 Probable reaction scheme in the hydrogenation of BN. Benzonitrile (BN), benzylamine (BA), benzylideneimine (BI), α -aminodialkylamine (BIBA), *N*-benzylidenebenzylamine (DBI), dibenzylamine (DBA), and toluene (TOL)

rise of the BN/H_2 molar ratio (1:8), both conversion of BN and selectivity of BA are raised. At 1:12 molar ratio, a downfall in the conversion of BN (78%) was noticed, while the selectivity of BA increased to 68%. The selectivity of BA is increasing with the BN/H_2 molar ratio. There exists a competition between H_2 , BN, and BA

Table 2 Comparison of Ni/MgO catalyst activity with reported catalytic systems

Catalyst	Reaction conditions				BN Conv. (%)	BA Sel. (%)	References
	Solvent	Temp. (K)	Additive	Pressure of H ₂ (bar)			
Pd-MCM-41	–	323	–	20	91	90	[14]
Ni/Mo	Methanol	378	NH ₃ /H ₂ O	41	100	99	[21]
RuCl ₂ (PPh ₃)	Toluene	353	^t BuOK	50	98	98	[9]
Pd/Al ₂ O ₃	2-Propanol	353	–	10	100	95	[10]
Pd/ γ -Al ₂ O ₃	Ethanol	343	–	15	100	86	[16]
Ni/MgO	–	473	–	1	98	60	Present study

to adsorb onto active sites. At low BN/H₂ mole ratio, the available active sites are more and the formed BA product could adsorb and participate in further hydrogenolysis reactions to form TOL so that the selectivity to BA is decreased. As the BN/H₂ molar ratio increases, the available active sites for BA to adsorb and participate in reactions are less. Hence, the selectivity to BA is more at high BN/H₂ molar ratio.

To explore the catalyst stability of 10Ni/MgO catalyst, it is subjected to time-on-stream (TOS) studies, and results are presented in Fig. 9. On continuous study of 36 h, the 10Ni/MgO catalyst is stable with consistent activity and selectivity which shows the sturdiness of the catalyst. The catalytic activity of Ni/MgO catalyst is compared with reported catalytic systems and presented in Table 2. It illustrates that 10Ni/MgO catalyst is free from additives, noble metal catalysts, and pressurized operations.

Conclusions

Ni/MgO catalysts were prepared by co-precipitation method and used for hydrogenation of benzonitrile to benzylamine in continuous process at atmospheric pressure. All the Ni/MgO catalysts are found to be active and selective for the production of benzylamine from hydrogenation of benzonitrile. 10 wt% Ni/MgO catalyst exhibited better performance with 98% conversion of benzonitrile and 60% selectivity to benzylamine without using any additives and mild reaction conditions. The high dispersion of Ni and strong metal support interactions with MgO are key factors for the catalytic performance. 10 wt% Ni/MgO catalyst is robust during 36-h life study.

Acknowledgements AN thanks CSIR-New Delhi, India, for the award of fellowship.

References

1. S.A. Lawrence, *Amines: Synthesis, Properties and Applications*, vol. 1 (Cambridge University Press, Cambridge, 2004)
2. H.A. Wittcoff, B.G. Reuben, J.S. Plotkin, *Industrial Organic Chemicals* (Wiley, New York, 2005)

3. K. Weisserme, H.J. Arpe, *Industrial Organic Chemistry* (Wiley, Wenham, 2003)
4. R.K. Marella, K.S. Koppadi, Y. Jyothi, K.S. Rama Rao, B. David Raju, *New J. Chem.* **37**, 3229 (2013)
5. S. Das, S. Zhou, D. Addis, S. Enthaler, K. Junge, M. Beller, *Top. Catal.* **53**, 979 (2010)
6. K. Lévay, L. Hegedűs, *Periodica Polytechnica Chem. Eng.* **62**(4), 476 (2018)
7. S. Enthaler, D. Addis, K. Junge, G. Erre, M. Beller, *Chem. Eur. J.* **14**, 9491 (2008)
8. L. Hegedus, T. Mathe, *Appl. Catal. A* **296**, 209 (2005)
9. S. Enthaler, K. Junge, D. Addis, G. Erre, M. Beller, *Chem Sus Chem.* **1**, 1006 (2008)
10. Y. Cao, L. Niu, X. Wen, W. Feng, L. Huo, G. Bai, *J. Catal.* **339**, 9 (2016)
11. Y. Cao, H. Zhang, J. Dong, Y. Ma, H. Sun, L. Niu, X. Lan, L. Cao, G. Bai, *Mol. Catal.* **475**, 110452 (2019)
12. H. Yoshida, Y. Wang, S. Narisawa, S.I. Fujita, R. Liu, M. Arai, *Appl. Catal. A* **456**, 215 (2013)
13. A.J. Yap, A.F. Masters, T. Maschmeyer, *Chem. Catal. Chem.* **4**, 1179 (2012)
14. Y.L.D. Jesus, C. Johnson, J. Monnier, C. Williams, *Top. Catal.* **53**, 1132 (2010)
15. M. Chatterjee, H. Kawanami, M. Sato, T. Ishizaka, T. Yokoyama, T. Suzuki, *Green Chem.* **12**, 87 (2010)
16. O.Q. Dominguez, S. Martinez, Y. Henriquez, L.D. Ornelas, H. Krentzien, J. Osuna, *J. Mol. Catal. A* **197**, 185 (2003)
17. D. Chengyong, Z. Shuya, W. Xueguang, Z. Chunlei, Z. Wenxiang, L. Yonggang, C. Ning, *New J. Chem.* **413**, 758 (2017)
18. H. Cheng, X. Meng, C. Wu, X. Shan, Y. Yu, F. Zhao, *J. Mol. Catal. A* **379**, 72 (2013)
19. Y. Hao, M. Li, F. Cardenas-Lizana et al., *Catal. Lett.* **146**, 109 (2016)
20. C. Dai, F. Liu, W. Zhang, C. Li, Y. Ning, X. Wang, C. Zhang, *Appl. Catal. A Gen.* **538**, 199 (2017)
21. M.S. Wainwright, *Preparation of Solid Catalysts* (Wiley, Weinheim, 1999)
22. D. Ostgard, M. Berweiler, S. Roder, *US Patent A1* **017**, 3676 (2002)
23. R.A. Plunkett, J.L. Neff, T. Bemish, *US Patent* **025**, 4163 (1979)
24. F.M. Cabello, D. Tichit, B. Coq, A. Vaccari, N.T. Dung, *J. Catal.* **167**, 142 (1997)
25. X. Chen, X. Wang, S. Yao, X. Mu, *Catal. Commun.* **39**, 86 (2013)
26. V. Mohan, V. Venkateswarlu, B. David Raju, K.S. Rama Rao, *New J. Chem.* **40**, 3261 (2016)
27. V. Mohan, V. Venkateswarlu, C.V. Pramod, B. David Raju, K.S. Rama Rao, *Catal. Sci. Technol.* **4**, 1253 (2014)
28. Q. Shi, C. Liu, W. Chen, *J Rare Earths* **27**, 948 (2009)
29. M. Jafarbegloo, A. Tarlani, A.W. Mesbah, *Catal. Lett.* **146**, 238 (2016)
30. H. Chen, M. Xue, J. Shen, *Catal. Lett.* **13**, 246 (2010)
31. A. Zecchina, G. Spoto, S. Coluccia, E. Guglielminotti, *J. Chem. Soc. Faraday Trans.* **80**, 1875 (1984)
32. A. Kuzmin, N. Mironova, *J. Phys. Condens. Matter.* **10**, 7937 (1998)
33. Y.H. Wang, H.M. Liu, B.Q. Xu, *J. Mol. Catal. A Chem.* **299**, 44 (2009)
34. L. Yanrong, L. Gongxuan, M. Jiantai, *RSC Adv.* **4**, 17420 (2014)
35. R.A. Plunkett, J.L. Neff, T. Bemish, *US Patent* **025**, 4163 (1979)

Publisher's Note Springer Nature remains neutral with regard to jurisdictional claims in published maps and institutional affiliations.